Journal of Structural Engineering

Comparison of Tests of a Nonlinear Structure Using a Shake Table and the EFT Method

Jian Zhao, M. ASCE[1], Catherine French, M. ASCE[2],
Carol Shield, M. ASCE [3], and Thomas Posbergh[4]

ABSTRACT: The viability of effective force testing (EFT), a real-time dynamic testing procedure for large-scale structures, has been validated by comparing results of tests on idealized structural models to analytical results. In this paper, the results of tests on a shake table are compared to those conducted using the EFT method. The test structure was a one-story steel structure consisting of typical structural components. The paper also presents an overview of critical issues required for conducting the EFT test, and highlights many problems and solutions that may affect the performance of EFT tests. The comparison of the test results indicates that with proper velocity feedback compensation, the EFT method can be used to apply real-time seismic simulation to structures undergoing nonlinear deformation.

CE Database subject headings: Effective force testing; Dynamic tests; Test procedures; Earthquake engineering; Servomechanisms.

INTRODUCTION

Real-time dynamic testing is a powerful tool for investigating the behavior of structural systems under seismic loading, especially for studying structures employing strain-rate critical components and structures incorporating velocity dependent devices

[1] Assistant Prof., Dept. of Civil Eng. & Mech., Univ. of Wisc. – Milwaukee, WI. E-mail: jzhao@uwm.edu
[2] Prof., Dept. of Civil Eng., Univ. of Minnesota, Minneapolis, MN. E-mail: cfrench@umn.edu
[3] Associate Prof., Dept. of Civil Eng., Univ. of Minnesota, Minneapolis, MN. E-mail: ckshield@umn.edu
[4] Associate Prof., Dept. of Electrical and Computer Engineering, Univ. of Minnesota, Minneapolis, MN. E-mail: posbergh@umn.edu

(e.g. semi-active or passive damping devices). Shake tables can be used to simulate the dynamic effects of earthquakes on structures, but size limitations often mandate the use of reduced scaled structural models.

Effective force testing (EFT) is a dynamic testing technique that overcomes many of the limitations of a shake table, while using common laboratory equipment (i.e., servo-hydraulic actuators). The EFT Method was first conceived by Mahin and his co-workers (Mahin & Shing 1985; Mahin et al. 1989; Thewalt & Mahin 1987), and initially evaluated and implemented at the University of Minnesota by Dimig et al. (1999). This testing technique can be used to perform dynamic tests on structures that can be idealized as lumped-mass systems. The development to date has been mainly focused on single-degree-of-freedom (SDOF) systems. Given an SDOF model of a structural system subjected to base acceleration ($\ddot{x}_g$), the equation of motion can be stated as

$$m\ddot{x} + c\dot{x} + kx = -m\ddot{x}_g = P_{eff} \,, \tag{1}$$

where *m*, *c*, and *k* are the structural mass, damping and stiffness, and x, $\dot{x}$, and $\ddot{x}$ are the structural displacement, velocity, and acceleration relative to the base, respectively (Chopra, 1995). In an EFT test, the test structure is anchored to a stationary base, and dynamic forces ($P_{eff} = -m\ddot{x}_g$) are applied by a hydraulic actuator to the center of the structural mass. Hence, if the force applied to the structure (effective force) were exactly the ground acceleration times the structure mass, motions measured relative to the ground would be equivalent to the structural response that a structure would develop relative to a moving base as in a shake table test or an earthquake event.

An EFT system is schematically shown in Figure 1 and its block diagram is shown in Figure 2(a). The electro-hydraulic actuator is in force control (i.e., command signals to

the servovalve are based on the difference between command forces and measured forces). Because the interaction between the actuator piston velocity and actuator control affects the operation of the actuator with a standard PID controller (Dyke et al. 1995), a velocity feedback compensation loop is required to ensure forces to be applied to the structure accurately (Dimig et al. 1999). The velocity feedback compensation loop, shown in dashed lines in both figures, modifies the command signal sent to the servovalve controller based on **measured** velocity (Shield et al. 2001). In practice, additional hardware (e.g., a digital controller board and a velocity transducer) need to be used to implement the velocity feedback compensation (Zhao et al. 2002).

The velocity feedback compensation as shown in Figure 2(a) must incorporate the inverse of the forward system dynamics (i.e., the dynamic properties of the servovalve and its controller) to properly modify the command signal to the servovalve. When large forces and/or large velocities are involved in a test, a large amount of flow is necessary to conduct the test. In these cases significant nonlinearities exist in the servovalve behavior, and the nonlinearities can have an impact on the performance of the test system (Zhao et al. 2003a and 2003b). Hence, nonlinear velocity feedback compensation implemented using a digital signal controller is necessary (Zhao et al. 2005).

This paper presents an experimental validation of EFT following a brief review of the nonlinear velocity feedback compensation. A one-story building structure consisting of typical structural components was tested using a shake table and the EFT method. Forces (effective forces and applied forces) and structural responses are compared to demonstrate the feasibility of EFT in testing structures undergoing nonlinear deformations. Problems encountered during the investigation are explored to facilitate

future applications of EFT.

EFFECTIVE FORCE TESTING

The laboratory implementation of the EFT method requires velocity feedback compensation to accurately control the actuator. The compensation signal needs to be modified by the inverse of the forward system dynamics as shown in Figure 2(a) before being added to the effective force command signal. Hence, the system needs to be characterized before a test.

System Characterization

The forward system dynamics contain three major components as shown in Figure 2(b): (1) the proportional-integral-derivative (PID) control with a zero I gain,

$$H_c = \frac{v}{e} = G_p + G_d s, \tag{3}$$

where G_p and G_d are the proportional and derivative gain of controller, respectively; (2) the second-order servovalve dynamics,

$$H_s = \frac{x_v}{v} = \frac{K_s}{\frac{1}{\omega_v^2} s^2 + \frac{2\zeta_v}{\omega_v} s + 1}, \tag{4}$$

where K_s is the valve gain and ω_v and ζ_v are the equivalent natural frequency and damping of the servovalve respectively.; and (3) the nonlinear servovalve flow relationship stated by

$$Q_L = K_v x_v \sqrt{1 - \frac{x_v}{|x_v|}\frac{P_L}{P_s}}, \tag{5}$$

where x_v is the spool opening of the servovalve, K_v is the no-load flow gain of the servovalve, which is a function of spool opening, P_L is the load pressure ($P_L A$ is

approximately the force applied to the structure, and A is the actuator piston area), and P_s is the supply pressure. Note that the servovalve flow relation includes two types of nonlinearity: the **load pressure influence** expressed by the square root term and the **nonlinear no-load flow gain** (K_v), which is defined using a piece-wise linear curve as shown in the following parameter identification section.

Velocity Feedback Compensation

The velocity feedback compensation was implemented in this study using a dSpace DS1102 DSP controller with a TI TMS320C31 floating-point digital signal processor with a 2 kHz sampling rate. The digital controller board was hosted in a personal computer. The effective force command signal (after being converted into a voltage signal) was an input to the DSP board through an on-board A/D converter. Three other analog signals were also input to the DSP board: 1) measured structural velocity, 2) valve spool opening, and 3) the applied force as measured by the actuator load cell. The three later inputs were manipulated by the nonlinear velocity compensation algorithm shown next, and then added to the effective force command to form the modified command signal. The new command was then sent out through an on-board D/A converter to the input port of the servovalve controller.

The nonlinear velocity feedback compensation algorithm is shown in Figure 2(b). The compensation signal, defined as measured structural velocity (input 1) multiplied by the actuator piston area (A), which was obtained from the product specification, was first multiplied by $1\Big/\sqrt{1-\frac{x_v}{|x_v|}\frac{P_L}{P_s}}$ to consider the effect of large forces applied to the structure. This process required the hydraulic supply pressure (assumed constant) and two more inputs, the spool opening (x_v) and the load pressure (P_L). The spool opening (input 2) was

obtained directly from the servovalve controller while the load pressure was approximated by the applied force (input 3) divided by the piston area (A). The hydraulic supply pressure was taken as the average value read from the service manifold during the parameter identification tests. A look-up table, defining the servovalve flow property (K_v) as shown in the Parameter Identification section, was then used to determine the required spool opening that would provide the compensation flow to the actuator.

The major effect of the servovalve dynamics (H_s) on the velocity feedback compensation is the response delay of the servovalve (T_d) for low frequencies (i.e., 0-10 Hz in this study). Hence, the compensation signal (the above required spool opening divided by the valve gain (K_s)) was further modified by a first-order phase-lead algorithm to counteract the response delay as shown in Figure 2(b). In the process, the time constant (T_{ld}) was calculated as $T_d/(1-\alpha)$, and α was taken as 0.1 (Zhao et al. 2003a).

Finally, the PID control setting was optimized through linear system analysis along with trial tests as discussed in the Parameter Identification Section. A zero I-gain and a small D-gain (a fraction of a millisecond) were used, and the P-gain took the maximum allowable value as described in the next section. The inverse of the controller dynamics (H_c) was simplified as the reciprocal of the controller P-gain (G_p). The compensation was multiplied by $1/G_p$ before added to the effective force command.

The implementation of the above algorithm in C language can be found elsewhere (Zhao, 2003). Shown below is the determination of the three critical parameters for the implementation of the nonlinear velocity feedback compensation. These parameters are the nonlinear flow property of the servovalve, the servovalve response delay, and the controller P gain for the servo-system used in this study.

Identification of Critical Parameters

In this study, the effective forces were applied to the structure by a 156-kN (35-kip) MTS 244.52 actuator. The actuator was powered by a 341 lpm (90-gpm) MTS 256.09 servovalve, which was in turn controlled by an MTS 407 analog controller. The hydraulic supply was provided by two 284 lpm (75-gpm) pumps. The average supply pressure observed throughout the study was 20 MPa (2850 psi).

Servovalve flow property: The flow property defines the flow controlled by the servovalve to the actuator (Q_L) corresponding to a spool opening (x_v). A piecewise linear curve (i.e. the aforementioned look-up table) was constructed using results of a series of tests with 3 Hz sinusoidal displacement commands. The actuator was detached from the structure in these tests, resulting in negligible pressure difference across the actuator piston (the load pressure $P_L = 0$). Because the square root term in Eq. (5) is equal to 1.0 in this case, the flow was calculated by the piston velocity multiplied by the piston area. The piston velocity was calculated from the measured piston displacement using the central difference method.

Tests with 90% (4.5 in.), 80% (4 in.), 60% (3 in.), 40% (2 in.), and 20% (1 in.) full stroke command were conducted. The tests generate data for 21 control points at an interval of 10% spool opening for the Q_L-x_v curve. The flow values at the control points were calculated as the average value of all test results at that spool opening. Figure 3 compares the piecewise linear flow curve to the test result with the 90% full stroke command. It is noted that the measured flow property of the servovalve (as shown by the grey dots) is scattered about the piecewise linear approximation, indicating some possible instantaneous over-or under- compensation for the natural velocity feedback when the

compensation is based on the identified flow curve.

Servovalve response delay: The servovalve response delay (T_d) was estimated based on the second-order model of the servovalve shown in Eq. (4). To experimentally evaluate the parameters in the model, another test was conducted with sine wave sweep valve commands. In this test, the actuator was in displacement control, and the actuator piston was kept in its neutral position by turning off the hydraulic supply to the main-stage valve. In addition, the proportional gain of the servovalve controller was set to unity, and the derivative gain set to zero.

A sine wave sweep (0-100 Hz in 100 sec) equivalent to 20% spool opening was chosen as the input signal (i.e., displacement commands with 25-mm (1-in) amplitude for the actuator used in this study). The system output, spool opening, was obtained through the servovalve controller. The obtained frequency response is shown in Figure 4 along with the simulation results using Eq. (4). The valve gain (K_s) was found to be 0.1 from the amplitude response. A frequency of 57.5 Hz and a damping of 80% fit the phase response well, from which the response delay was found to be 4.4 ms for low frequencies. It should be noted that the servovalve dynamics can be affected by system nonlinearities, and the response delay increases with an increase in the hydraulic demand. To account for this increase, a response delay of 5 ms was found to be appropriate for this study through a series of EFT tests with small amplitude sine sweep inputs.

Controller P gain: A Proportional-Integral-Derivative (PID) controller was used to improve the performance of the servo-system. A standard tuning procedure as shown in the product specification was followed to determine the controller gain settings. In addition, it was noticed that I-gain is typically used to improve the steady-state behavior

of a system while capturing the transit behavior of the structure is the goal of the study; hence a zero I-gain was used in this study. Also because the derivative control component amplifies high-frequency noise, the D-gain was kept small (a fraction of a millisecond).

Relatively large P-gains should be used because they usually improve the overall performance of a stable system (Franklin et al, 1994). On the other hand, larger controller P-gains may cause system instability, resulting in a high-frequency component in the force applied to the structure. Such unstable system response was observed several times during the study. A linear stability analysis of the test system applying Routh's stability criterion (Franklin et al, 1994) was used to estimate the range for setting the controller P gain. Detailed analysis can be found elsewhere (Zhao 2003). In addition to the system analysis, the P-gain was finalized as 1.0 during the series of EFT tests with small amplitude sine sweep inputs used to determine the servovalve response delay.

With these parameters identified, the EFT method with the nonlinear velocity feedback compensation was applied to a one-story steel structure, and the results were compared to those from a companion shake table study.

EXPERIMENTAL PROGRAM

Test Structure

A simple one-story structure was selected for the study, which consisted of a rigid diaphragm (a rectangular steel frame filled with reinforced concrete) supported on four replaceable steel columns at its corners as shown in Figure 6. The shake table study was conducted at the University of Illinois at Urbana-Champaign, and the EFT test was conducted at the University of Minnesota using the same test structure. The concrete mass, which weighed about 4,590 kg (10 kips), was selected to fit the load capacity of the

shake table, and the column spacing, 1.5×1.8 meters (60×72 inches), was selected to fit the hole-pattern of the base plate on the shake table.

The columns were made of W10x15 section (A572 grade 50 steel) with a reported yield stress of 431 MPa (62.5 ksi). The columns were 1.8 m (72 inch) high and oriented in weak-axis bending such that the resonant frequency of the structure was low enough to be excited by most earthquake ground acceleration records. The bending stiffness in the orthogonal direction was much larger (20 times) than that in the loading direction such that out-of-plane motion was prevented without additional diagonal braces. The middle chevron brace connected to two fluid dampers by Taylor Devices Inc. to limit the structural responses such that tests could be repeated and results compared before testing the structure into the nonlinear range of behavior. The dampers also introduced nonlinearities to the structure in the tests shown in the Experimental Results Section.

The structural properties were found similar between the two test setups as shown in Table 1. With data from two free-vibration tests, the structural properties were determined through parametric simulations, which minimize the error between the measured displacements and simulation results based on a least square technique. Both viscous damping and Coulomb friction were considered in the simulations. The stiffness during the EFT tests was 1% greater than that in the shake table study due to a slight change in base plates and column boundary condition. The structural mass increased by 2% during the EFT tests, which was in part due to the addition of a thick plate for connecting the actuator. Hence, the natural frequency of the structure in the two studies changed by approximately 1% (from 2.89 Hz in the shake table study to 2.87 Hz in the EFT study). The damping change is relatively larger (from 9.6% equivalent viscous

damping in the shake table study to 8.2% in the EFT study), which was attributed to an unknown change in the dampers and a change in test environment. With reduced damping, it was anticipated that the displacement and velocity of the structure in the EFT study would be slightly greater than those in the shake table study.

Data Reduction

Both global and local responses of the structure were monitored. The measured global responses included acceleration, velocity, and displacement of the mass. All global measurements in the EFT study were relative responses. In the shake table tests, the acceleration and displacement were relative to the global reference; hence, the table movement was subtracted from the measured responses to obtain the relative responses to the table for comparison. The monitored local responses for both test methods included column flange strains and damper forces. Strain gages were placed on each flange tip 0.2 m (8 inches) from the column ends. The column moment was calculated from strain measurements assuming an elastic-perfectly plastic response, and the column base shear was calculated by dividing the sum of the two measured column moments by the distance between the gage sections.

Input Ground Motions

The input ground motions used in the shake table study included a sine wave sweep acceleration record (1-10 Hz), an El Centro earthquake ground acceleration record (Imperial Valley earthquake on May 18, 1940, recorded at 270 degrees with a 0.35g peak ground acceleration), and a Northridge earthquake ground acceleration record (January 17, 1994, recorded at Santa Monica City Hall at 90 degrees with a 0.84g peak ground acceleration). In the shake table tests, the acceleration signals were transformed into

required displacement signals by the actuator controller through double integration. To keep the table within its stroke limits, the sine sweep inputs ranged between 1 Hz to 10 Hz , and the maximum peak ground accelerations for El Centro and Northridge earthquakes were limited (0.30g and 0.55g, respectively). For the companion EFT tests, the **measured** table acceleration multiplied by the estimated structural mass was used as the effective force command because the table did not follow commanded signals perfectly.

EXPERIMENTAL RESULTS

Shown in Figures 6 through 10 is a comparison of the results obtained in the EFT study and the companion shake table study. Note that when forces are compared, the label "Shake table test" indicates the measured table acceleration times the estimated structural mass, which was also the effective force command for the EFT tests; the label "EFT test" indicates the force applied to the structure measured by the actuator load cell.

Tests with Two Dampers (8% damping)

Tests were conducted first with two dampers attached to the chevron brace. The results with a 0.55 g Northridge earthquake input are presented in Figures 6 and 7. Only 10 seconds of response (from 6 to 16 sec) are shown to make the graphs more readable. The force comparison in Figure 6 shows that the effective force command was followed by the actuator closely in the EFT test. The Fourier amplitude of the force applied to the structure by the actuator was slightly greater than the force command in the frequency domain, indicating a slight overcompensation of the natural velocity feedback due to uncertainties in the estimation of the servovalve flow property. Both the global responses

(displacement, velocity, and acceleration) and local response (column base shear) of the EFT test compared well to those of the shake table test as shown in Figure 7. The structural responses obtained during the EFT test were slightly greater than those of the shake table test, which was attributed to the slight overcompensation of the natural velocity feedback and the decrease in structural damping. In addition, the after-shock free vibration, which began at 15 sec, was accurately captured.

The measured damper behavior shown in Figure 8 indicates that the damper forces were not proportional to the velocity (i.e., dampers were not ideally viscous), which introduced nonlinearities to the test structure. Two such dampers were connected as shown in Figure 5 to provide a symmetric damping (equivalent to 8% of critical damping). The maximum spool opening in the test was approximately 25%, which was beyond the linear range (10%) of the servovalve performance (refer to Figure 4).

Tests without Dampers (0.25% damping)

Tests using the EFT method on to the structure without the dampers were problematic as shown by the first 12 sec of the test with the El Centro earthquake in Figure 9, which compares the measured force in the EFT test with the 0.3g El Centro earthquake effective forces input. Although the actuator seemed able to follow the force command in the time domain, large force overshoots are evident in the frequency domain. The system was driven into the unstable region after 4 sec, and the structural responses were much larger than those obtained in the shake table study as shown in Figure 10.

The unstable system was attributed to the use of a predetermined flow curve in the velocity feedback compensation, which does not account for the uncertainties of the hydraulic system as shown in Figure 4. The system uncertainties may have caused

instantaneous overcompensation, which in turn may have caused instability of the test system. The test structure without the dampers had very little damping (approximately 0.25% of critical damping), such that the test system was not able to tolerate the instantaneous instability. An attempt was made to prevent the unstable system behavior through reducing the natural velocity feedback compensation. Although the system stability was achieved by eliminating the instantaneous overcompensation, the force applied to the structure, especially near the natural frequency of the structure, was reduced, and the structural responses were smaller than those obtained in the shake table study as a result.

Tests with Other Damping Ratios

Tests with one Taylor damper were conducted without encountering a stability problem. The damper provided an equivalent damping of 4% though the damper performance was asymmetric as shown in Figure 8. To further explore the system stability in testing the structure with smaller damping, two automobile shock absorbers were used to replace the Taylor dampers towards the end of the study. As shown in Figure 11(a), the automobile shock absorbers provided three times more damping force in the negative direction than in the positive direction. With the damper configuration shown in Figure 2 to counteract the asymmetry, the equivalent damping based on a free vibration test was 2.3%. The system was stable during the EFT tests.

The measured force applied to the structure is compared in the frequency domain with the command force in Figure 11 (b). The comparison indicates that the actuator was able to apply forces at all frequencies within 10 Hz. A small amplitude drop around 3 Hz (the natural frequency of the test structure) is evident, which might have been due to the

aforementioned system uncertainties not included in the velocity feedback compensation. Therefore, it appears that a structure having at least 2% damping can be tested using EFT with the current velocity feedback compensation scheme without experiencing problems associated with instantaneous instability. The peak displacement observed, 42 mm (1.65 in), was much large than the predicted yield displacement (19 mm (0.75 in)). In addition, the maximum spool opening was 55%, which is beyond the linear range of servovalve behavior. These observations indicate that with nonlinear velocity feedback compensation, the EFT method can be used to test nonlinear structures with large hydraulic demands.

PROBLEMS ENCOUNTERED

The performance of the EFT method with the current velocity feedback compensation scheme requires an accurate knowledge of the servovalve and its controller. Servo-system uncertainties, such as leakage and pressure supply variation, reduce the accuracy of the system identification, thus affecting the laboratory implementation of the velocity feedback compensation. A variety of problems were explored as follows.

Leakage Flow

The servo-system leakage is caused by hardware wear and manufacturing imperfections. The leakage, including the servovalve leakage and actuator internal and external leakage, affects the stability and controllability of the servovalve/actuator. Part of the servovalve and actuator leakage is proportional to the load pressure (referred to as the proportional leakage hereafter), and can add damping to the test system, which allows an increased controller P gain as indicated by linear system analysis with a reasonable

estimation of the leakage coefficient (Zhao et al, 2005).

Over the course of the study, the servo-system leakage was found to be large due to two heavily worn low pressure seals on the actuator. Consequently, the actuator was sent to the manufacture for repair. The refurbishment greatly reduced the proportional leakage, such that the controller P gain had to be set low, which affected the performance of the test system. An external leakage passage was created by connecting the two ports to the actuator chambers with a controllable needle valve. With an increased proportional leakage, the unity controller P gain could be used during the study, which improved the behavior of the test system to produce the plots presented in this paper.

Pressure Supply Variation

Two hydraulic pumps provided 568 lpm (150 gpm) hydraulic fluid flow with 20 MPa (2850 psi) pressure (measured at the service manifold near the actuator used in this study). When the actuator drew hydraulic flow from the supply line and drove roughly the same amount of flow into the return line, the flow consumption caused a pressure drop in the supply line. The pressure reduction in the supply line was sensed and compensated by the hydraulic pumps. Because the hydraulic pumps had their own dynamics and response delay, the pressure supply to the servovalve varied during the tests, which was believed to be one cause for the variation in the measured servovalve flow property.

The supply pressure variation was not compensated in the laboratory. Typical pressure gages have response times much longer than the refreshing time of the velocity feedback compensation. In addition, the measure supply pressure using a pressure gage coupled in the hydraulic supply line can not exactly represent the pressure inside the

actuator (P_s). The resulted modeling error might be significant enough to result in a poor response of the test system. An accumulator with a capacity of 0.004 m^3 (¼ gallon) closely coupled to the servovalve was used to reduce the uncertainty of the supply pressure to the servovalve. In addition, an average measure pressure was used as the supply pressure in the inverse relation of the load pressure influence. The average supply pressure was evaluated during the tests for identifying the servovalve flow gain (K_v), which required large flow demand similar to that could be expected in the EFT tests.

Velocity Measurement

The measured velocity might include unwanted signals, including electrical noise and the vibration of the sensor support. The noise can be amplified through the velocity feedback compensation because the compensation signal is added to the effective force command. It was found that velocity measurement near the actuator swivel head could cause an unstable vibration with a high frequency (Timm, 1999). In this study, the velocity sensor was placed on the opposite side of the structure from the actuator as shown in Figure 1 to avoid the problem. However, the reference column of the velocity sensor was first rigidly attached to the ground, which transmitted vibrations caused by the actuator acting against the strong wall/floor system. The noisy velocity feedback signal caused the application of a high-frequency force component to the structure, such that the force measurement was very noisy even though the structure was not excited at that frequency (i.e., it was far from the natural frequency of the structure).

Filtering the high frequency signals was inappropriate because the filtering process would introduce phase delay to the velocity signal, which would deteriorate the velocity feedback compensation. Instead, a rubber sheet placed underneath the reference column

of the velocity sensor was used to isolate the sensor from the ground to solve the problem.

CONCLUSIONS

This study demonstrated the feasibility of EFT by presenting the comparison of tests of a one-story steel structure using a shake table and the EFT method. The comparison of the test results showed that the EFT method can accurately apply real-time seismic simulation to structures. The nonlinear velocity feedback compensation scheme used requires an accurate model of the servovalve; however, accurate identification of the related parameters is difficult because of inherent uncertainties in the system. For the test structure to tolerate possible instantaneous overcompensation of the natural velocity feedback due to the servo-system uncertainties, the test structure should have at least 2% of critical damping to avoid instability.

A variety of problems that could affect the performance of the EFT method were explored. The potential problems investigated included uncertainties in the servo-system (i.e., extensive leakage flow and pressure supply variation) or errors in velocity measurement caused by actuator dynamics. The leakage flow affects the system controllability and stability and can be evaluated by observing the servovalve/actuator performance. The pressure variation can be measured using pressure gages and the problem may be solved by coupling a large size accumulator in the system. In addition, a more advanced adaptive velocity feedback compensation scheme may be necessary to compensate for these issues while the problems associated with the velocity measurement can be resolved by carefully selecting the velocity sensor position. As researchers employ

the EFT method for structural testing, the capabilities of existing laboratory equipment will expand to real-time dynamic testing. The investigation of these potential problems should prove useful to those future implementations.

ACKNOWLEDGEMENTS

Funding for this research was provided by the National Science Foundation (NSF) under grant number: CMS-9821076. The Doctor Dissertation Fellowship provided by the 3M Corporation through the Graduate School at the University of Minnesota is also acknowledged. Information contained herein does not necessarily represent the views of the sponsors.

APPENDIX I. REFERENCES

1. Chopra, A. K. (1995). *Dynamics of structures: Theory and applications to earthquake engineering*. Prentice-Hall, Englewood cliffs, N.J.

2. Dyke, S. J., Spencer, B. F., Quast, P., and Sain, M. K. (1995). Role of control-structure interaction in protective system design. *Journal of Engineering Mechanics*, ASCE, 121(2), 322–338.

3. Dimig, J., Shield, C., French, C., Bailey, F., and Clark, A. (1999). Effective force testing: A method of seismic simulation for structural testing. *Journal of Structural Engineering*. 125(9), 1028-1037.

4. Mahin, S. A. and Shing, P. B. (1985) Pseudodynamic method for seismic testing. *Journal of Structural Engineering.* 111, 1482-1503.

5. Mahin, S. A., Shing, P. B., Thewalt, C. R. and Hanson, R. D. (1989) Pseudodynamic test method| current status and future directions. *Journal of Structural Engineering 115, 2113-2128.*

6. Franklin G.F., Powell J.D., and Emami-Naeini A. (1994). *Feedback control of dynamic systems.* (3rd edition) Addison-Wesley, Boston, MA.

7. Shield, C., French, C., and Timm, J. (2001). Development and implementation of the Effective force testing method for seismic simulation of large-scale structures. *Philosophical Transaction of the Royal Society: Theme Issue on Dynamic Testing of Structures*; A 359: 1911-1929.

8. Timm, J. (1999). *Natural velocity feedback correction for effective force testing*. Master's thesis, Civil Engineering, University of Minnesota, Minneapolis.

9. Thewalt, C. R. and Mahin, S. A. (1987) Hybrid solution techniques for generalized pseudodynamic testing. Report UBC/EERC-87/09, EERC, University of California, Berkeley, USA.

10. Zhao J., French C., Shield C., and Posbergh T. (2002). Development of EFT for nonlinear SDOF systems. *Proc. 7th National Conf. on Earthquake Engineering*. Boston, MA,

11. Zhao J., French C., Shield C., and Posbergh T. (2003a). Nonlinear velocity compensation for Effective Force Testing. *Proc. 2003 Structural Congress and Exhibition*. Seattle, WA

12. Zhao J., French C., Shield C., and Posbergh T. (2003b) Considerations for the development of real-time dynamic testing using servo-hydraulic actuation. *Earthquake Engineering and Structural Dynamics*. Vol. 32, No. 11. pp. 1773-1794.

13. Zhao J., Shield C., French C., and Posbergh T. (2005). Nonlinear System Modeling and Velocity Feedback Compensation for EFT. *Journal of Engineering Mechanics* ASCE, 131(3), 244–253.

14. Zhao, J. (2003). *Development of EFT for Nonlinear SDOF Systems*, Ph.D. thesis, Civil Engineering, University of Minnesota, Minneapolis.

APPENDIX II. NOTATION

The following symbols are used in this paper:

A	Actuator piston area
e	Error signal in servovalve control
G_p	Proportional gain setting of the PID controller
G_d	Derivative gain setting of the PID controller
H_c	Servovalve controller dynamics
H_s	Servovalve dynamics
K_s	Servovalve gain
K_v	Valve flow gain
m, c, k	Structural parameters
P_{eff}	Effective force
P_L	Load pressure (pressure difference across the actuator piston)
P_s	Hydraulic pressure supply
Q_l	Hydraulic flow to the actuator
s	Variable in the frequency domain
T_d	Servovalve response delay
T_{ld}	Lead time in the phase-lead network
v	Command signal to the servovalve
$x,\ \dot{x},\ \ddot{x}$	Structural responses
$\ddot{x}_g$	Ground acceleration
x_v	Servovalve spool opening
α	Constant used in the phase-lead network
ω_v	Apparent natural frequency of the servovalve
ζ_v	Equivalent damping of the servovalve

Table 1 Structural properties

	Shake table test			Effective force test		
	damping kN-s/m	friction N	stiffness kN/m	damping kN-s/m	friction N	stiffness kN/m
no damper	0.53	4.45	1510	0.35	4.45	1533
w/ damper	15.42	35.6	1510	13.84	0	1519

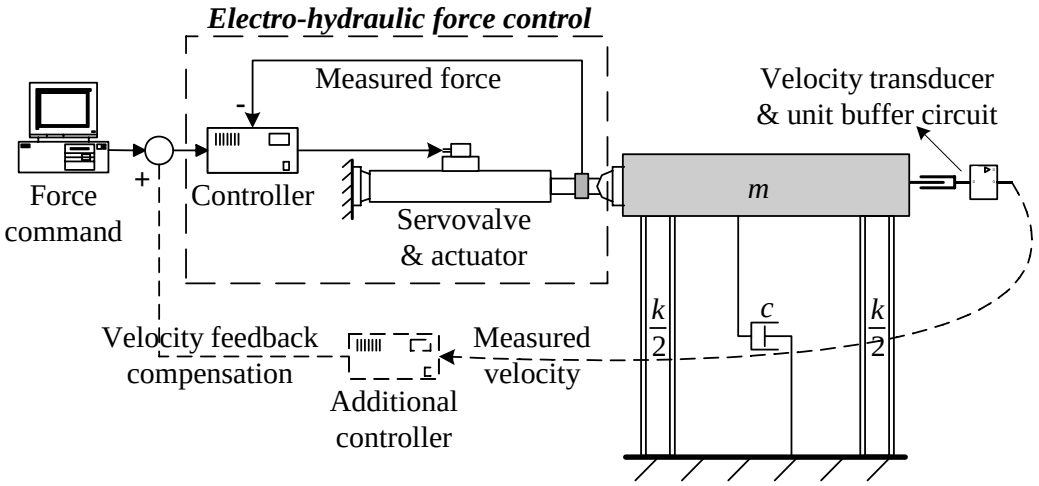

Figure 1 Schematics of an EFT system with SDOF structure

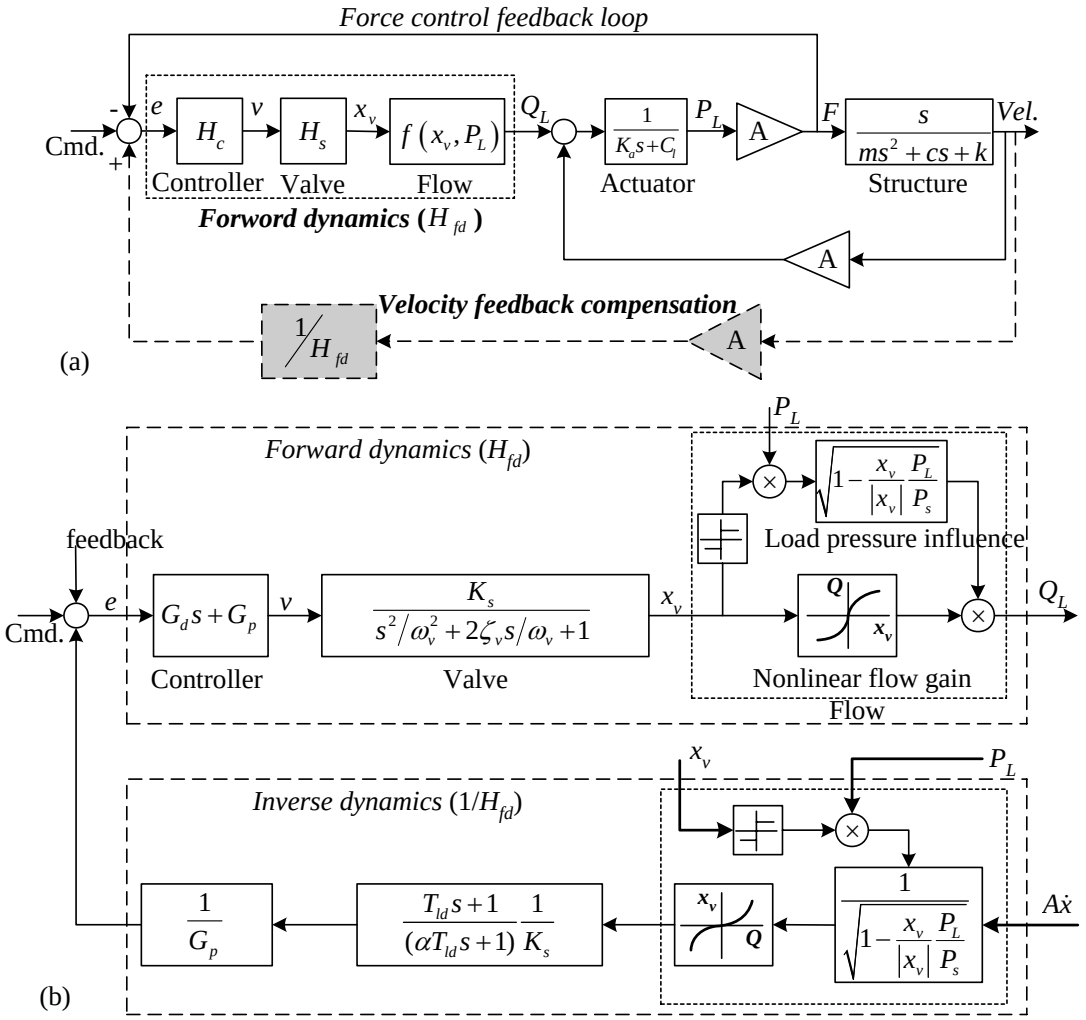

Figure 2 Block diagram of the EFT system. (a) Overall testing system; (b) Nonlinear velocity feedback compensation

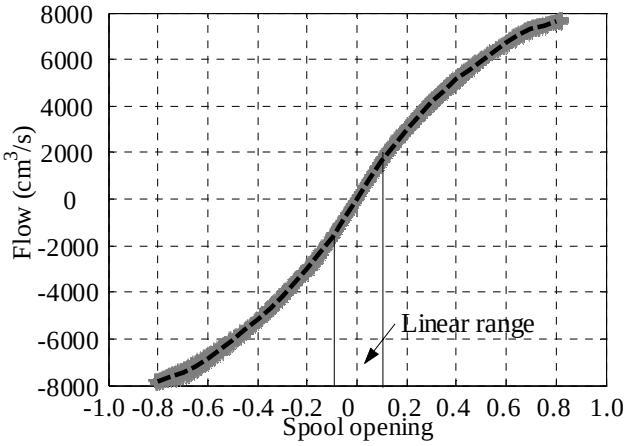

Figure 3 Servovalve no-load flow property

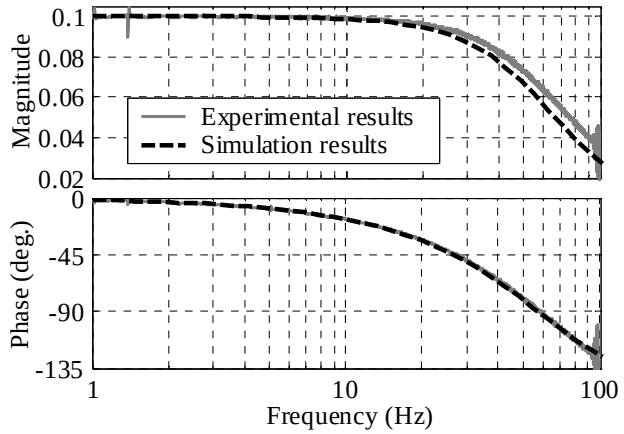

Figure 4 Measured servovalve dynamics

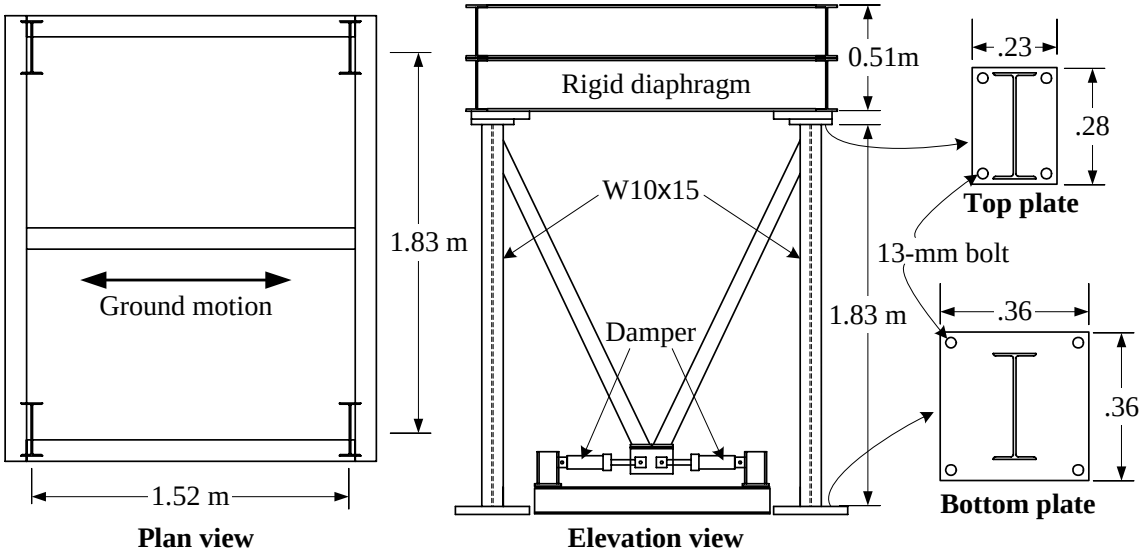

Figure 5 One-story test structure

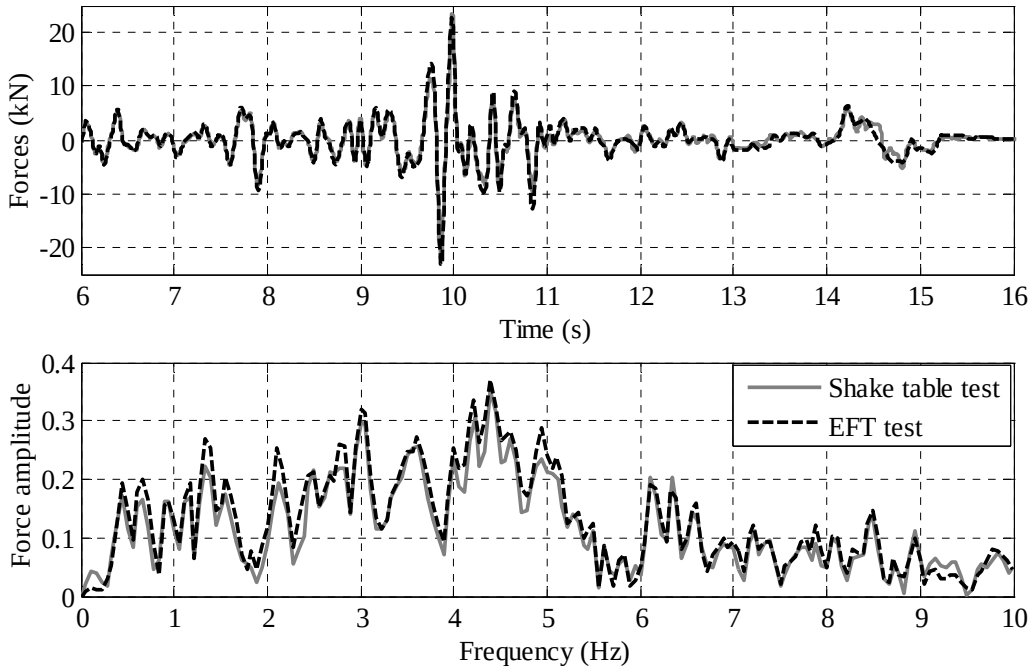

Figure 6 Comparison of effective forces and the force output of the test with two dampers and 0.55g Northridge earthquake

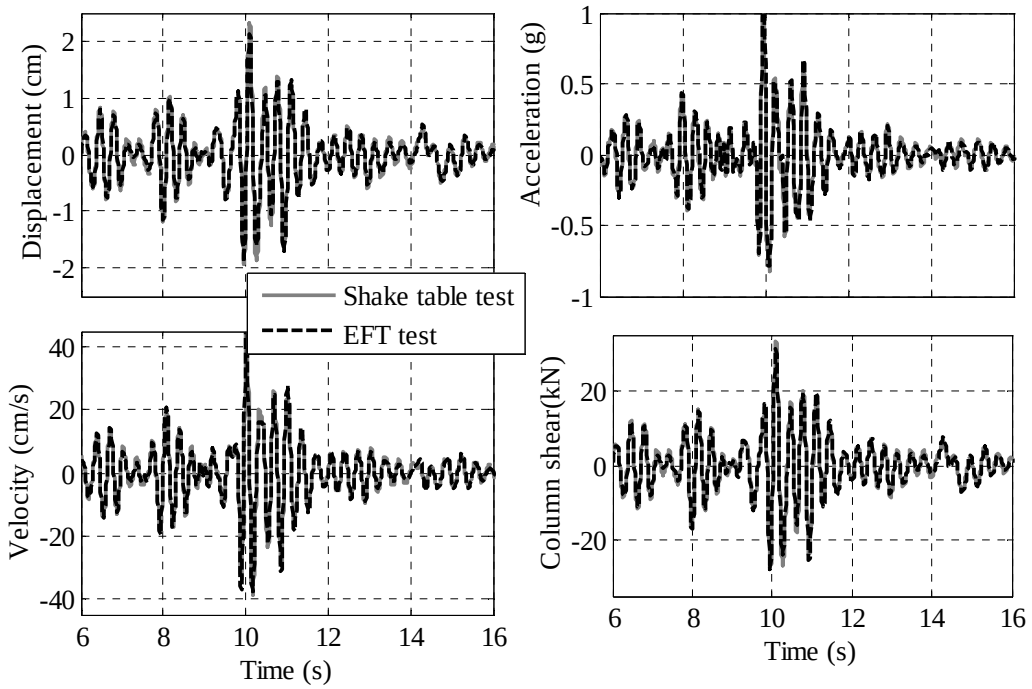

Figure 7 Comparison of structural responses of the test with two dampers and 0.55g Northridge earthquake

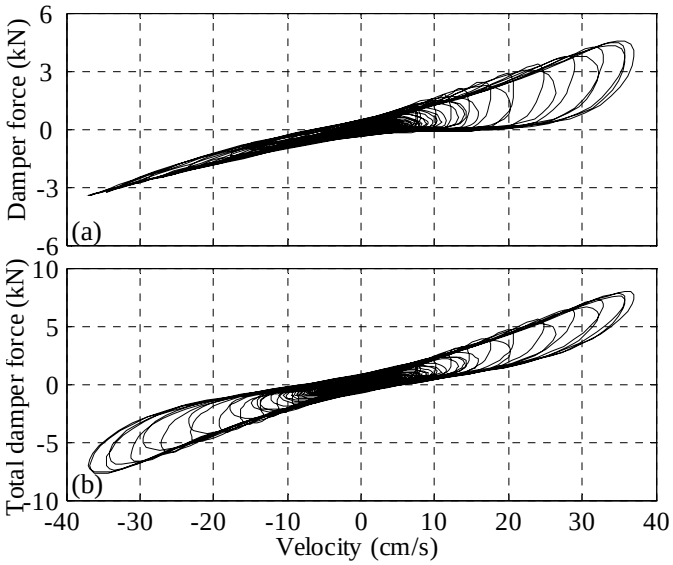

Figure 8 Performance of Taylor dampers. (a) Single damper case; (b) Two damper case

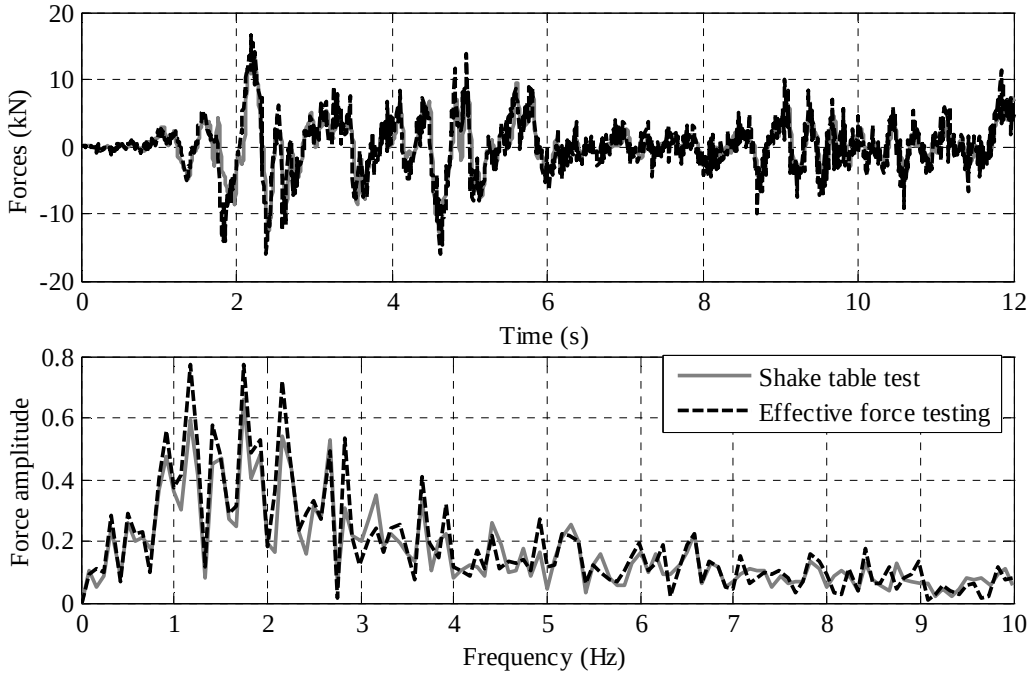

Figure 9 Comparison of effective forces and the force output of the test without dampers and 0.3g El Centro earthquake

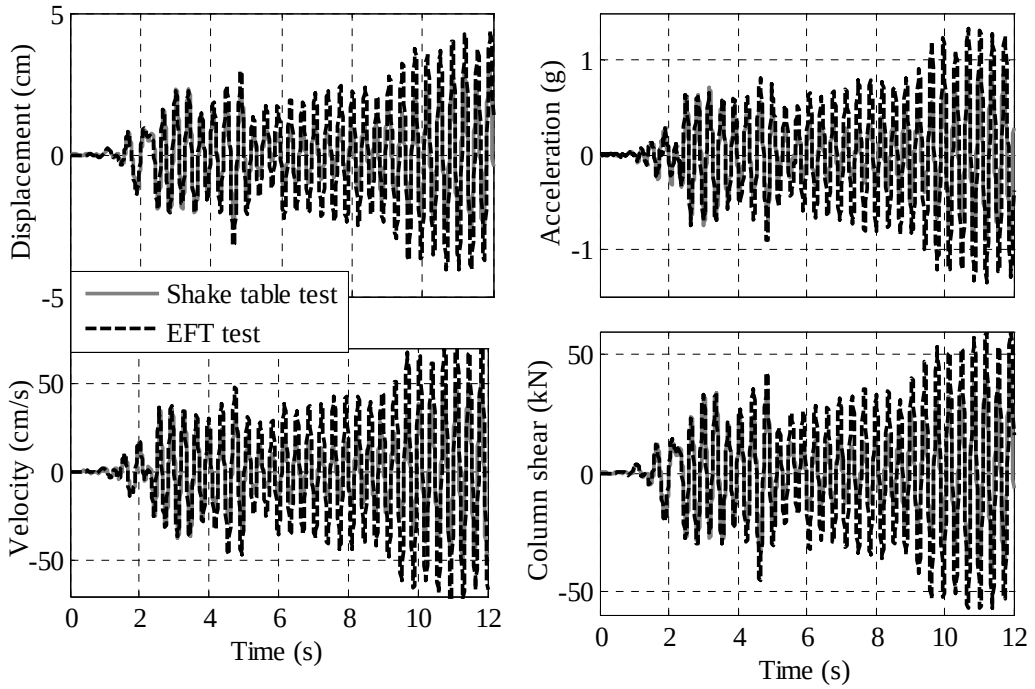

Figure 10 Comparison of structural responses of the test without dampers and 0.3g El Centro earthquake

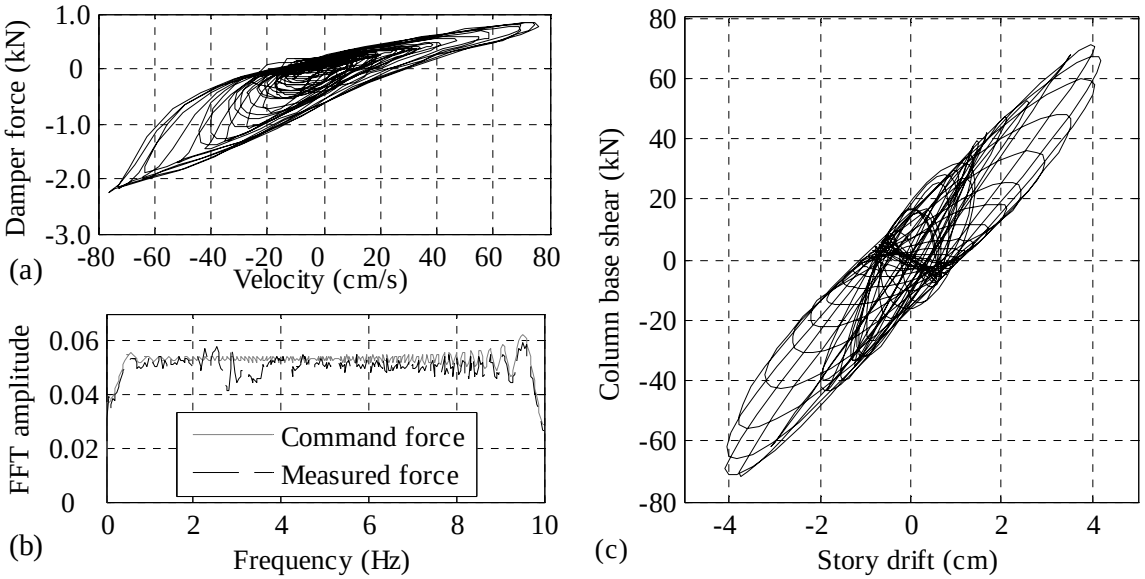

Figure 11 (a) Performance of a single automobile shock absorber; (b) Comparison of applied forces and command forces in the test with two automobile shock absorbers (2% damping) and 2 kip sinesweep input; (c) Structural nonlinearity during the test